Accuracy of Probabilistic Harmonic Estimation in Sparsely Monitored Transmission Networks

DOI:
10.1109/PMAPS53380.2022.9810613

Accuracy of Probabilistic Harmonic Estimation in Sparsely Monitored Transmission Networks

Yuqi Zhao, Jovica V. Milanović
the University of Manchester
Manchester, UK
yuqi.zhao@postgrad.manchester.ac.uk
jovica.milanovic@manchester.ac.uk

Pablo Rodríguez-Pajarón, Araceli Hernández
Universidad Politécnica de Madrid
Madrid, Spain
pablo.rpajaron@upm.es
araceli.hernandez@upm.es

***Abstract*— Accurate estimation of harmonics in uncertain, power electronics interfaced large transmission networks without installation of excessive number of power quality monitors can significantly improve and facilitate the probabilistic harmonic propagation studies. Traditional harmonic state estimation methods have been widely studied but are still very challenging in practical application due to the requirement of a large number of synchronized monitoring devices and real-time operational structure of the network. Based on a preliminary study that demonstrates the effectiveness of sequential artificial neural networks (ANNs) in the probabilistic harmonic estimation in uncertain transmission networks, this paper presents further comprehensive accuracy assessment in terms of different types/numbers of harmonic measurements, different stop errors to optimise training time and limited numbers of installed power quality monitors due to realistic reasons. It has been demonstrated that the sequential ANNs is sufficiently accurate and applicable in estimating harmonics in uncertain transmission network, thus contributing to facilitate the identification of potential harmonic issues, benchmarking, standard compliance and the deployment of appropriate harmonic propagation and mitigation solutions.**

***Keywords*— ANN, harmonic estimation, renewable energy source, sparsely monitored transmission system, uncertainties**

I. Introduction

Power system harmonic distortions are highly associated with the increasing penetration level of power electronic (PE) devices, e.g., renewable generations. In response to the global environmental-friendly policies, there are more and more PE interfaced devices continuously connecting into the large transmission system, leading to additional uncontrolled harmonic power flows and unexpected harmonic issues, thus resulting in significant financial loses to both transmission system operators (TSOs) and customers [1, 2].

Accurate estimation of harmonic propagations is one of the feasible options to effectively anticipate and mitigate the harmonic problems. As a traditional solution, the harmonic state estimation (HSE) method [3-5] have been widely studied. For example, in the area of proposing optimal monitor-placement methods [6] and combining with ANN-based techniques to improve the estimation precision and accelerating convergence [7-10]. However, for a typical large transmission system which is sparsely monitored and highly dynamic and uncertain in nature, the HSE method is still very challenging in practical application since it requires adequate synchronized monitoring devices, specific parameters of the system topology at the and real-time operational structure of the network [3-5].

A sequential ANNs method [11] has been proposed for reliable estimation of probabilistic harmonic distortions at unmonitored buses in large uncertain transmission networks. As an extension study, this paper evaluates the effectiveness of the sequential ANNs and presents further comprehensive accuracy assessment considering the effect of different types and length of harmonic measurements utilised for training, the effect of amplifying stop errors to optimise training time and the effect of decreasing the number of installed power quality monitors/monitored buses in the large transmission system due to the financial and technical reasons.

The test network is modelled and simulated in the DigSILENT/PowerFactory environment [12], using Monte Carlo based probabilistic approach for considering operating uncertainties caused by PE interfaced generation and non-liner loads [13, 14]. The sequential ANNs was implemented in MATLAB. All the trainings are performed using a personal computer with Intel® Core™ i7-4770 CPU @ 3.4GHz.

II. Methodology

A. Harmonic Estimation

In this study, a sequential ANNs method, introduced in [11], is utilised for the estimation of harmonic distortions in a transmission network, where limited number of harmonic monitoring devices are installed and limited number of harmonic orders are measured. The method combines the successive application of two different two-layer feed-forward neural networks namely ANN1 and ANN2. Similar to the structure introduced in [15-17], ANN1 is a neural network with m input-layer neurons (m represents for the number of monitored buses), 28 hidden-layer neurons and n output-layer neurons (n represents for the number of unmonitored buses). ANN2 is a neural network, and with h input-layer neurons (h represent for the total number of individual harmonic orders), 28 hidden-layer neurons and single output-layer neuron (represents for THD at an unmonitored bus). Both ANN models are trained using Levenberg-Marquardt Backpropagation (LMBP) training function [18]. The transfer functions of the hidden and output layer are log-sigmoid and tan-sigmoid, respectively. The block diagram of entire THD estimation methodology is shown in Fig. 1.

ANN1 aims to estimate individual harmonic distortions (h^{th} order) of the target week at all unmonitored buses (the output) based on h^{th} harmonic measurements at the monitored

This work was partly supported by Grant RTI2018-097424-B-I00 funded by MCIN/AEI/10.13039/501100011033 and by "ERDF A way of making Europe".

978-1-6654-1211-7/22/$31.00 ©2022 IEEE

buses from the same week (the input). It has been trained using the h^{th} order of harmonic measurements of previous weeks at all the monitored buses, as the input and the h^{th} order harmonic measurements of previous weeks at all the unmonitored buses, as the target. According to the standard EN 50160 [19], only 2nd-25th harmonic are considered in this study.

ANN2 aims to estimate THD of the target week at all unmonitored buses based on all individual orders of harmonic distortions estimated by ANN1. It has been trained using individual harmonic distortions of previous weeks at the n^{th} unmonitored bus as the input, and the THD values of previous weeks at the n^{th} unmonitored bus as the target. The advantage of using a sequential ANNs method to estimate THD compared to more traditional approach that uses individual harmonics and conventional formula for calculating THD at unmonitored buses has been clearly demonstrated in [11].

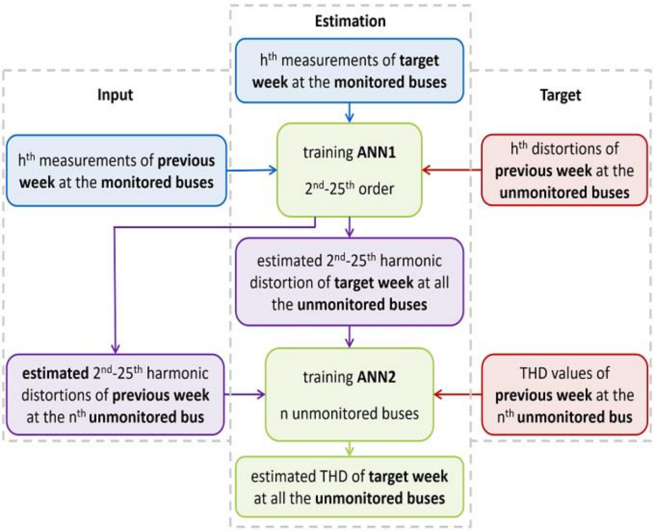

Fig. 1. Block diagram of THD estimation methodology (adopted from [11]).

When evaluating the accuracy of the probabilistic harmonic estimation method, the absolute error (AE), defined by (1) and the relative error (RE), defined by (2) are utilised.

$$absolute\ error = t_i - a_i \quad (1)$$

$$relative\ error = \frac{t_i - a_i}{a_i} * 100\% \quad (2)$$

where t_i and a_i stand for the estimated value and the actual value of a sample i, respectively.

B. Test Network

The database of harmonic measurements are obtained by performing harmonic load flow (HLF) in a modified IEEE 68-bus New England Test System-New York Power System (NETS-NYPS) test network (shown in Fig. 2). There are 16 synchronous generators (G1-G16), 20 renewable energy generations (10 wind farms and 10 PV plants) and a total of 35 loads (industrial type and distribution network (DN) type of loads) integrated in this system. Individual loads are modelled as a combination of linear and non-linear components (50% for industrial load, 20% for DN type of loads). The penetration level of RES is set as 60%.

C. Probablistic Modelling of Uncertainties and Harmonic Injections

One-week actual renewable generation profiles in Europe [20] are interpreted as probabilistic scaling factors in this study when modelling the system uncertainties regarding different operating conditions, e.g., varying loads, wind and PV outputs. According to standard IEEE519 [21], the probabilistic scaling factors are updated every 10-min interval. For loads, wind, and PV plans, the probabilistic output/loading scaling factors are assumed to be sampled by following Normal distribution (μ=1, σ=0.033). Weibull distribution (φ=11.1, k=2.2) and Beta distribution (α=13.7, β=1.3), respectively [14].

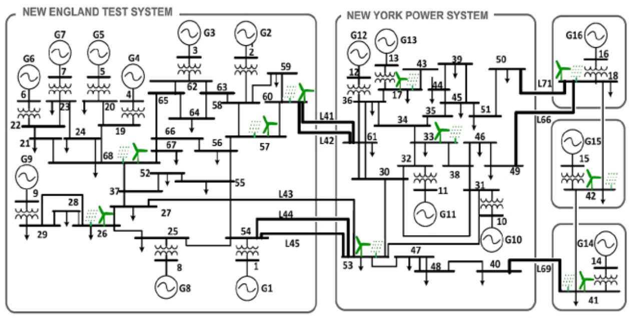

Fig. 2. Modified IEEE 68-bus NETS-NYPS test network.

In transmission network, harmonic distortions are mainly injected by PE interfaced wind, PV, and load demands. Therefore, these types of components are modelled as 3-phase unbalanced harmonic current sources with random magnitudes and phase angles which are probabilistically sampled from different pre-defined ranges. The ranges of harmonic magnitude injections (Normal distributed) are defined based on long–term measurements [13] of the harmonic spectrum in terms of different types of harmonic sources and individual harmonic orders (2nd-25th). The range of harmonic phase injection is defined as (0°, 180°), applicable for all types of harmonic sources [1, 22].

III. Case Study

Since the accuracy of this probabilistic harmonic estimation method has been validated by one-day harmonic measurements in a preliminary study [11], in this case, the time span for collecting samples has been expanded to one or more weeks, and the period of THD estimation has been extended to one week at the same time.

Taking the realistic circumstances into consideration, it is assumed that in the test network, the buses that are connected with conventional generations, renewable generations and both types of loads are being monitored (52 buses in total), while the other buses (16 buses in total) are unmonitored. This means that the input layer and output layer of ANN1 has 52 neurons and 16 neurons, respectively. At the same time, in ANN2, there are 24 neurons in the input layer and single neuron in the output layer.

A. Accuracy Based on One-week Measurements

In order to compare the accuracy of the sequential ANNs method when using different types of harmonic measurements, it is trained considering two cases. Case 1, were weekly variation in measured harmonic distortions, used to train ANN model, was relatively small, i.e., the level of harmonic distortion during the week was stable. Case 2, were weekly variation in measured harmonic distortions was relatively large. Then the obtained estimated THD values are compared against the harmonic measurements from each other week (mutual verification). In order to avoid the extreme circumstances caused by the uncertainties, it is a common practice to take the 95th percentile value of harmonics as a comparison [22]. The harmonic voltages are expressed as a percentage of the fundamental voltage.

For Case 1, the probability density functions (PDFs) of absolute and relative errors of 95th percentile estimated THD are fitted and plotted in Fig. 3 (a) and Fig. 3 (b), respectively. It can be seen that the mean values of fitted absolute and relative errors at different buses are all approximately concentrated at 0%. According to the distribution span of the fitted absolute error, i.e., ±0.2%, and the distribution span of the fitted relative error, i.e., ±10%, this indicates that if the actual THD at the unmonitored bus is 3%, the corresponding estimated value will be within a range from 2.8% to 3.2%, i.e., less than 10% of the actual THD values.

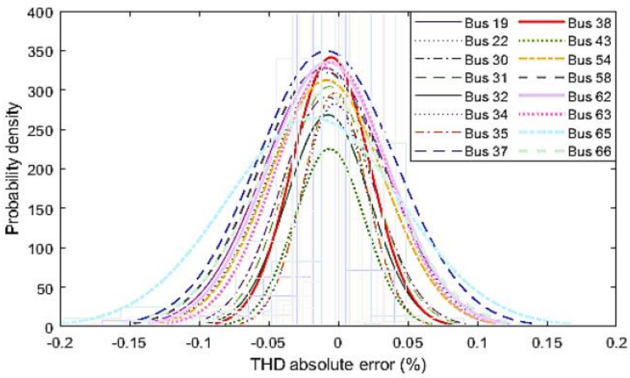

(a) PDFs of AEs of 95th percentile THD at unmonitored buses in Case 1.

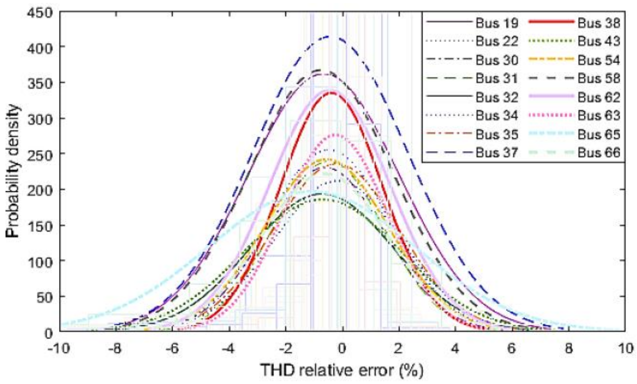

(b) PDFs of REs of 95th percentile THD at unmonitored buses in Case 1.

Fig. 3. Fitted PDFs of absolute error and relative error of the 95th percentile THD at unmonitored buses in Case 1.

For Case 2, Fig. 4 (a) and Fig. 4 (b) show the fitted PDFs and Normal-fitted cumulative distribution function (CDFs) of absolute errors of 95th percentile estimated THD, respectively. Fig. 5 (a) and Fig. 5 (b) show the fitted PDFs and CDFs of relative errors of 95th percentile estimated THD, respectively. It can be seen from the CDFs that during 90% of time the total absolute errors are less than 0.005%, and the total relative errors are less than 1%.

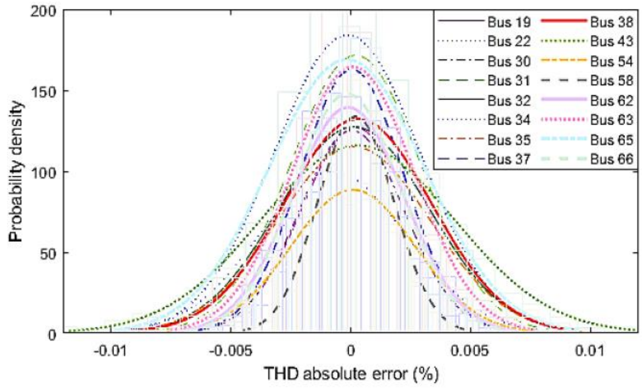

(a) PDFs of AEs of 95th percentile THD at unmonitored buses in Case 2.

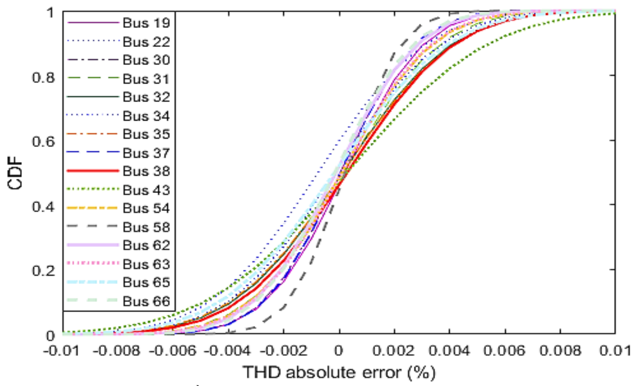

(b) CDFs of AEs of 95th percentile THD at unmonitored buses in Case 2.

Fig. 4. Fitted PDFs and CDFs of absolute error of the 95th percentile THD at unmonitored buses in Case 2.

Similar to Case 1, the mean values of fitted absolute and relative errors are all concentrated around 0%. However, the range of distributions of fitted absolute errors has been reduced significantly, i.e., from ±0.2% to ± 0.01%. The range of distributions of fitted relative estimation errors also deceased, approximately 5 times, from about ±10% to about ±2% of real measurements. This is because if the THD values are estimated based on a group of harmonic distortions measured when the system is stable, it is very challenging for the combined ANN model to predict unexpected fluctuations in a highly dynamic system due to the randomness and intermittence of RES. On the country, a group of volatile measurements would be able to accommodate extreme conditions and estimate THD values at unmonitored buses more accurately, regardless of various uncertain circumstances.

B. Accuracy Based on Multiple-weeks Measurements

In this case, the IEEE 68-bus NETS-NYPS test network is simulated again to obtain the harmonic measurements from a third week, which is considered as the comparison week. Then the combined ANN model is trained considering three cases, i.e., with less-variable weekly harmonic measurements (refer to as Case 3.1), with highly-variable weekly harmonic measurements (refer to as Case 3.2) and with measurement from both weeks (refer to as Case 3.3). Table I summarises the ranges of mean values and distributions of both fitted absolute and relative errors at all unmonitored buses, as well as the mean square errors (MSEs) of estimated THD at bus 19 (critical bus).

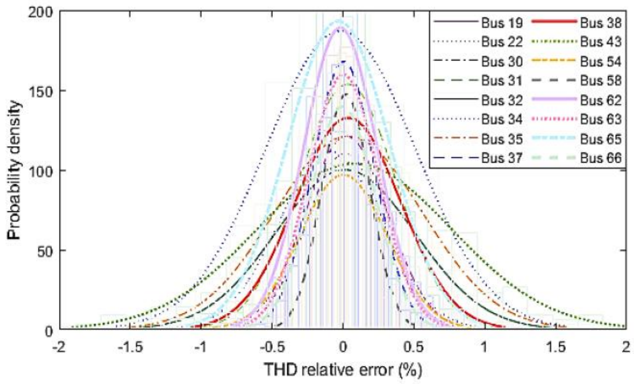

(a) PDFs of REs of 95th percentile THD at unmonitored buses in Case 2.

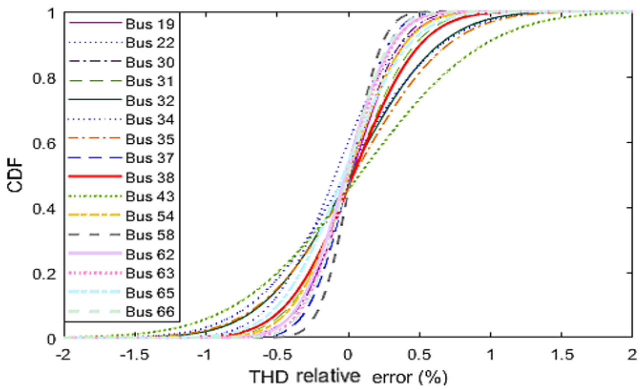

(b) CDFs of REs of 95th percentile THD at unmonitored buses in Case 2.

Fig. 5. Fitted PDFs and CDFs of relative error of the 95th percentile THD at unmonitored buses in Case 2.

It can be seen that for all three cases, the distributions of both absolute and relative errors are concentrated at approximately 0%, which confirms that the proposed model is sufficiently accurate in estimation THD at unmonitored buses. However, the distribution span of relative estimation errors and the MSEs at the critical bus tend to be smaller for Case 3.2 and Case 3.3 when a larger size of dataset is utilised to train the combined ANN model. This is because the larger dataset contains different operational uncertainties and is adequate to be compliant with a random week. However, the effect may not be so obvious since there are only one additional week considered in this case and there still exist random uncertainty.

TABLE Ⅰ
Comparison of the ranges of mean values and distributions of the fitted errors at all unmonitored buses and the MSEs at Bus 19.

	Case 3.1	Case 3.2	Case 3.3
Range of absolute mean value	0%	0%	0%
Range of absolute distribution	±0.71%	±0.23%	±0.24%
Range of relative mean value	0%	0%	0%
Range of relative distribution	±67.7%	±32.6%	±26.9%
MSEs at Bus 19	0.051	0.012	0.008

Fig. 6-8 illustrate the boxplots of the estimated and actual THD values on different unmonitored buses for Case 3.1-3.3, respectively. It can be seen that on the same bus, the medians, width and boundaries of boxplots are coincident with that of the actual THD boxplots. This indicates that for various unmonitored buses, the distributions of the predicted THD values correspond to their actual values, which further proves the general applicability of the combined ANN structure. However, in Fig. 6, it can be noticed that there are some outliners beyond the top of the box that are not able to be predicted. On the other hand, it can be seen from Fig. 7 and Fig. 8 that the outliners on the same unmonitored bus are approximately overlapped, which indicates that the extreme THD values can be accurately predicted. This may due to the fact that for Case 3.1, the measurement database used to train the combined ANN model is inclusive of different operation uncertainties and is adequate to be compliant with a random week, thus restraining the estimation errors.

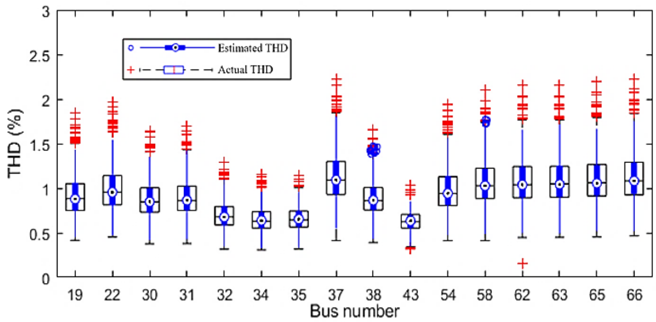

Fig. 6. Boxplots of estimated and actual THD values for different unmonitored buses for Case 3.1.

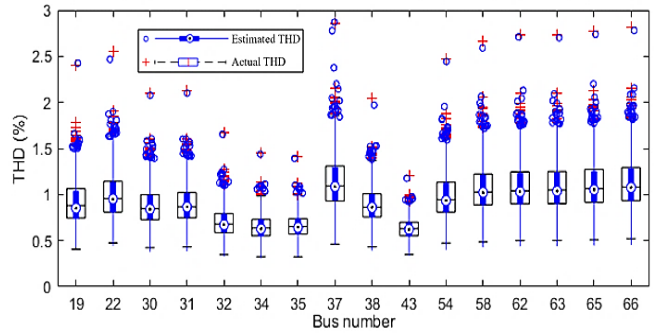

Fig. 7. Boxplots of estimated and actual THD values for different unmonitored buses for Case 3.2.

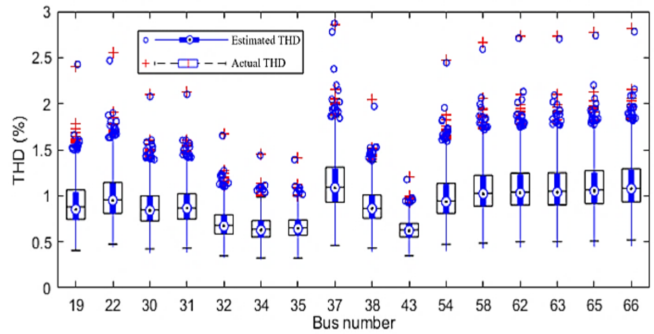

Fig. 8. Boxplots of estimated and actual THD values for different unmonitored buses for Case 3.3.

Therefore, when training the combined ANN model, it is recommended to consider highly-variable weekly/multi-weeks harmonic measurements if possible to take the uncertainties and contingency of system operations into consideration.

C. *Optimization of Training Time*

It has been noticed from the previous cases that with the increasing number of training samples, it takes longer to train the combined ANN model. As the main influence factor of training time, the training stopping error/threshold in ANN1 is increased to 10^{-2} in Case 4 to speed up the training process. The stopping criteria for training ANN2 though remained the same, i.e., 10^{-5}. After training combined ANN model, ANN1 takes approximately 24 hours less to train than in the Case 3.3.

Fig. 9 plots the CDFs of absolute prediction error of the 2nd-25th harmonics at Bus 19 of (a) Case 3.3 and (b) Case 4. It can be seen that during 90% of time, the total absolute errors of individual harmonics are less than 0.006%. When the stopping threshold in ANN1 is increased, the total absolute errors of individual harmonics during 90% of time are below with a range from -0.17% to 0.2%. Meanwhile, the span of fitted absolute errors become wider. Nonetheless, the estimation errors of individual harmonics are still within an acceptable range.

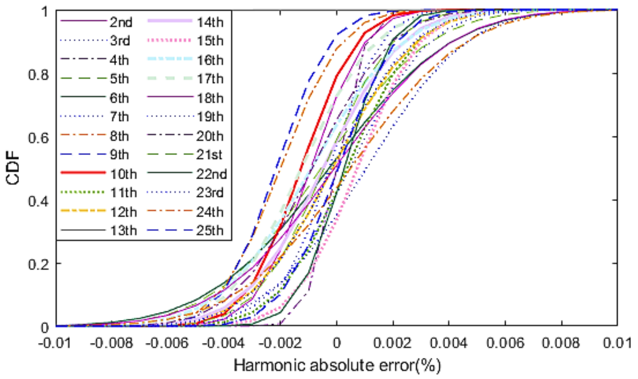

(a) CDFs of AEs of the 2nd-25th harmonics at Bus 19 in Case 3.3.

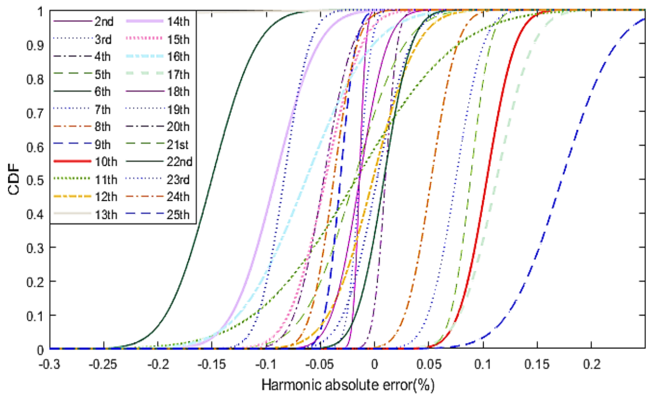

(b) CDFs of AEs of the 2nd-25th harmonics at Bus 19 in Case 4.

Fig. 9. Fitted CDFs of absolute prediction error of the 2nd-25th harmonics at Bus 19 in (a) Case 3.3 and (b) Case 4.

Table II summarises the ranges of mean values and distributions in PDFs of both fitted absolute and relative errors when estimating THD values at Bus 19. It can be seen that even though different stopping criteria were applied to ANN1, after training the ANN2, where the stopping threshold are sufficiently small, the estimated THD values on unmonitored buses still having the same level of accuracy.

Therefore, it is feasible to optimise the training time of ANN though changing stopping errors on the condition that the estimated errors of individual harmonic distortions are within acceptable limit. The requirement for the precision of estimated THD values on unmonitored buses can still be achieved through setting appropriate stop errors during the training of ANN2.

TABLE II
Comparison of the range of mean values and distributions of the fitted absolute and relative errors at Bus 19

	Case 3.3	Case 4	Case 5	Case 6
Mean value range of AE	0%	0%	±0.03%	±0.04%
Distribution range of AE	±0.24%	±0.21%	±0.24%	±0.21%
Mean value range of RE	0%	0%	±3.76%	±8.53%
Distribution range of RE	±26.9%	±24.3%	±28.2%	±31.11%

D. *Limited Number of Monitored Buses*

In order to investigate the accuracy of the estimation method in a sparsely monitored transmission network, different number and locations of monitored buses are assumed. For the purpose of saving the training time, the stopping errors of ANN1 and ANN2 are set as 10^{-2} and 10^{-5}, respectively. In Case 5, it is assumed that there are 34 buses being monitored and thus the other 34 buses are to be estimated. Taking the realistic circumstances in to consideration, the selected 34 monitored buses are the buses where synchronous generators, RES generators and industrial loads are connected. In Case 6, it is assumed that there are 18 monitored buses and thus the other 50 buses are to be estimated. The selected 18 monitored buses are those with RES generators and industrial loads connected to them.

In the sparsely monitored transmission network, as the number of unmonitored buses is increasing, more time is required to train the combined ANN model. In this case, the growth of training time is approximately in line with the cumulative number of unmonitored buses. For each additional unmonitored bus, it will take approximately extra two hours on average to train ANN1, and approximately extra 4.5 min on average to train ANN2.

Fig. 10 and Fig. 11 compare the boxplots of estimated and actual THD values for different unmonitored buses in Case 5 and Case 6, respectively. It can be seen that in both cases, the medians, width and boundaries of the estimated THD boxplots are coincident with that of the actual THD boxplots. The outliners on the same unmonitored bus are approximately overlapped, which indicates that the extreme THD values can be accurately predicted as well. The ranges of mean values and distributions of both fitted absolute and relative errors are also summarised in Table II. When there is a smaller number of monitored buses, the corresponding distributions of the absolute and relative estimation errors are roughly the same. There is up to approximately 0.04% increase in the mean value of fitted absolute errors and up to approximately 8.53% increase in the mean value of fitted relative errors, when the number of monitored buses drops from 34 (50% of all buses in the network) to 18 (26% of all buses in the network). This drop in accuracy generally can be considered as an acceptable considering the significant reduction in monitoring.

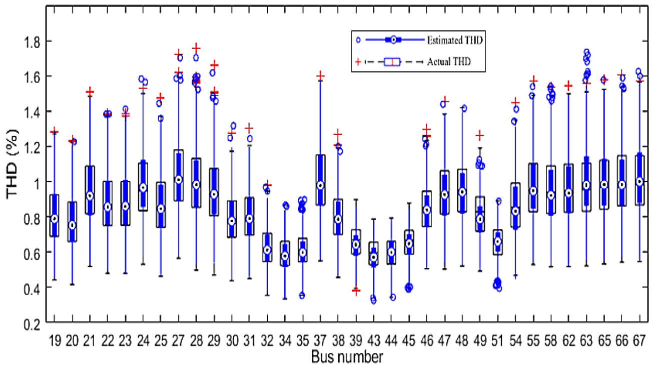

Fig. 10. Boxplots of estimated and actual THD values for different unmonitored buses for Case 5.

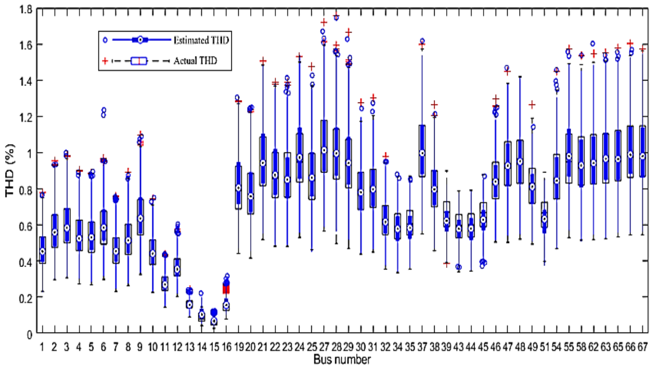

Fig. 11. Boxplots of estimated and actual THD values for different unmonitored buses for Case 6.

Therefore, the minimum number of buses that need to be monitored so that the established harmonic distortion values are within an acceptable limit of 10^{-2} is 18 buses. The number of monitored buses could be further reduced by setting smaller stopping errors at the expense of extended training time though.

IV. Conclusions

The paper evaluated the accuracy and effectiveness of using sequential ANNs for probabilistic estimation of harmonic distortions in sparsely monitored large transmission system considering the uncertainties introduced by increasing penetration level of power electronics interfaced renewable generations and nonlinear loads. The estimation accuracy is clearly established in terms of different types and length of harmonic measurements, different stopping thresholds/errors to optimise training time and limited numbers of installed power quality monitors. The presented accuracy assessment demonstrates that the proposed method is applicable and reliable tool to estimate harmonics under varying circumstances in large uncertain and sparsely monitored transmission networks. It could facilitate the identification of potential harmonic issues in the network and be applied for benchmarking and standard compliance purposes as well as to inform deployment of appropriate harmonic mitigation solutions.

Acknowledgment

This work was partly supported by Grant RTI2018-097424-B-I00 funded by MCIN/AEI/10.13039/501100011033 and by “ERDF A way of making Europe". This paper reflects only the author’s views and neither the Agency nor the Commission are responsible for any use that may be made of the information contained therein.

References

[1] Y. Zhao and J. V. Milanović, "Equivalent Modelling of Wind Farms for Probabilistic Harmonic Propagation Studies," in *IEEE Transactions on Power Delivery*, vol. 37, no. 1, pp. 603-611, Feb. 2022.

[2] G. J. Wakileh, *Power systems harmonics: fundamentals, analysis and filter design*. Springer Science & Business Media, 2001.

[3] S. K. Jain and S. Singh, "Harmonics estimation in emerging power system: Key issues and challenges," *Electric power systems research*, vol. 81, no. 9, pp. 1754-1766, 2011.

[4] A. S. Meliopoulos, F. Zhang, and S. Zelingher, "Power system harmonic state estimation," *IEEE Transactions on Power Delivery*, vol. 9, no. 3, pp. 1701-1709, 1994.

[5] X. Xiao, Z. Li, Y. Wang, and Y. Zhou, "A Practical Approach to Estimate Harmonic Distortions in Residential Distribution System," *IEEE Transactions on Power Delivery*, vol. 36, Jun. 2021.

[6] H. Liao, "Power system harmonic state estimation and observability analysis via sparsity maximization," *IEEE Transactions on Power Systems*, vol. 22, no. 1, pp. 15-23, 2007.

[7] S. K. Jain and S. Singh, "Fast harmonic estimation of stationary and time-varying signals using EA-AWNN," *IEEE Transactions on Instrumentation and Measurement*, vol. 62, no. 2, pp. 335-343, 2012.

[8] S. K. Jain and S. N. Singh, "Low-order dominant harmonic estimation using adaptive wavelet neural network," *IEEE Transactions on Industrial Electronics*, vol. 61, no. 1, pp. 428-435, 2013.

[9] H. Temurtas and F. Temurtas, "An application of neural networks for harmonic coefficients and relative phase shifts detection," *Expert Systems with Applications*, vol. 38, no. 4, pp. 3446-3450, 2011.

[10] A. Sarkar, S. R. Choudhury, and S. Sengupta, "A self-synchronized ADALINE network for on-line tracking of power system harmonics," *Measurement*, vol. 44, no. 4, pp. 784-790, 2011.

[11] Y. Zhao and J. V. Milanovic, "Probabilistic Harmonic Estimation in Uncertain Transmission Networks Using Sequential ANNs," *20th International Conference on Harmonics and Quality of Power (ICHQP)*, Naples, May, 2022.

[12] *DIgSILENT PowerFactory 2019 User Manual.* DIgSILENT GmbH, 2019.

[13] S. Abdelrahman, M. Wang, J. V. Milanović and E. Bećirović, "Study of harmonic propagation in transmission networks with high penetration of power electronics devices," *2017 IEEE Manchester PowerTech*, pp. 1-6, 2017.

[14] J. D. Morales and J. V. Milanović, "Methodology for Optimal Deployment of Corrective Control Measures to Ensure Transient Stability of Uncertain Power Systems," in *IEEE Transactions on Power Systems*, vol. 36, no. 3, pp. 1677-1687, May 2021.

[15] Y. Xu and J. V. Milanović, "Artificial-intelligence-based methodology for load disaggregation at bulk supply point," *IEEE Transactions on Power Systems*, vol. 30, no. 2, pp. 795-803, 2014.

[16] P. Rodríguez-Pajarón, A. H. Bayo and J. V. Milanović, " Forecasting voltage harmonic distortion in residential distribution networks using smart meter data," *International Journal of Electrical Power & Energy Systems*, vol. 136, pp. 107653, 2022.

[17] J. Ponoćko and J. V. Milanović, "Forecasting demand flexibility of aggregated residential load using smart meter data," *IEEE Transactions on Power Systems*, vol. 33, no. 5, pp. 5446-5455, 2018.

[18] S. O. Haykin, *Neural Networks and Learning Machines*, 3rd edition ed. Pearson Education, 2010.

[19] *Voltage characteristics of electricity supplied by public electricity*, EN standard 50160, 2010.

[20] [online] Available: https://open-power-system-data.org/.

[21] *IEEE Recommended Practices and Requirements for Harmonic Control in Electrical Power Systems*, IEEE Standard 519, 2014.

[22] Y. Zhao and J. V. Milanović, "Validation of the Equivalent Model of Wind Farm for Probabilistic Harmonic Propagation Studies," *26th International Conference and Exhibition on Electricity Distribution (CIRED 2021)*, 2021.